8

Modeling in Non–Equilibrium Thermodynamics

Preview

Until now, we have dealt with applications from either classical mechanics or electrical circuits exclusively. In this chapter, we shall discuss non–equilibrium state thermodynamics. Most engineering students consider thermodynamics a rather difficult topic. The reason for this seeming difficulty lies in the fact that basically all available treatises of thermodynamics have been written by *physicists* rather than by *engineers*. Physicists are, by education, *phenomenologically* rather than *systemically* oriented. They do not wish to change the world, only to understand it. Therefore, their approach to dealing with problems is quite different from ours. Rather than looking at a system as a whole and trying to analyze the couplings of its subsystems (as we engineers do), they always try to single out individual phenomena and discuss those in isolation. As a consequence, most physics texts present the topic through a collection of various formulae which are all individually correct and meaningful, but which are hard to relate to each other. It is the aim of this chapter to bridge the gap between those individually well–known equations that govern the behavior of non–equilibrium state thermodynamic systems. According to Jean Thoma, another reason why most thermodynamics textbooks are obscure is the fact that they avoid to work with *entropy flow* as a physical variable. He remarks rightly that textbooks for electrical circuit theory would be equally obscure if they were to describe all electrical phenomena in terms of the electrical potential and the stored energy alone while avoiding the concept of current flow [private communication]. In this text, thermodynamic phenomena will be described through a set of adjugate variables comparable to those used in electrical circuits and in mechanical motion.

8.1 Energy Flow

Traditionally, two separate approaches have been used for dealing with thermodynamics, a *macroscopic* approach that describes thermodynamics through variables such as *temperature*, *heat*, and *energy*, and which is deterministic in nature [8.7,8.17], and a *microscopic* approach that analyzes the movement of particles, and which is stochastic in nature [8.8,8.9,8.15]. In this text, we deal with the macroscopic, and therefore deterministic aspects of thermodynamics exclusively. For this purpose, we shall employ the bond graph methodology once more that was introduced in the previous chapter. It turns out that this methodology can present us with a good insight into the macroscopic processes that govern thermodynamic systems.

Let us start by revealing one more property of the bond graph approach to modeling which is related to the flow of energy.

Let us perform the following experiment. We take the simple electrical circuit drawn in Fig.8.1,

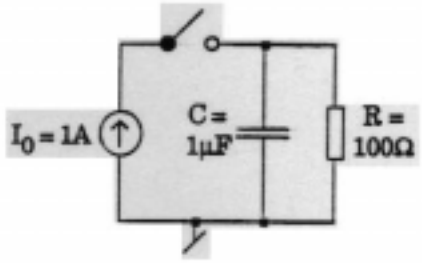

Figure 8.1. Simple RC circuit

and simulate this circuit during 0.5 *msec*. During the first 0.3 *msec*, the switch is closed, thereafter it is open. We coded this problem in ACSL (a trivial exercise). The results of the simulation are shown in Fig.8.2. From Fig.8.2, we see that the capacitor is being *charged* whenever the current and the voltage (proportional to the charge) have the same sign, and it is being *discharged* otherwise.

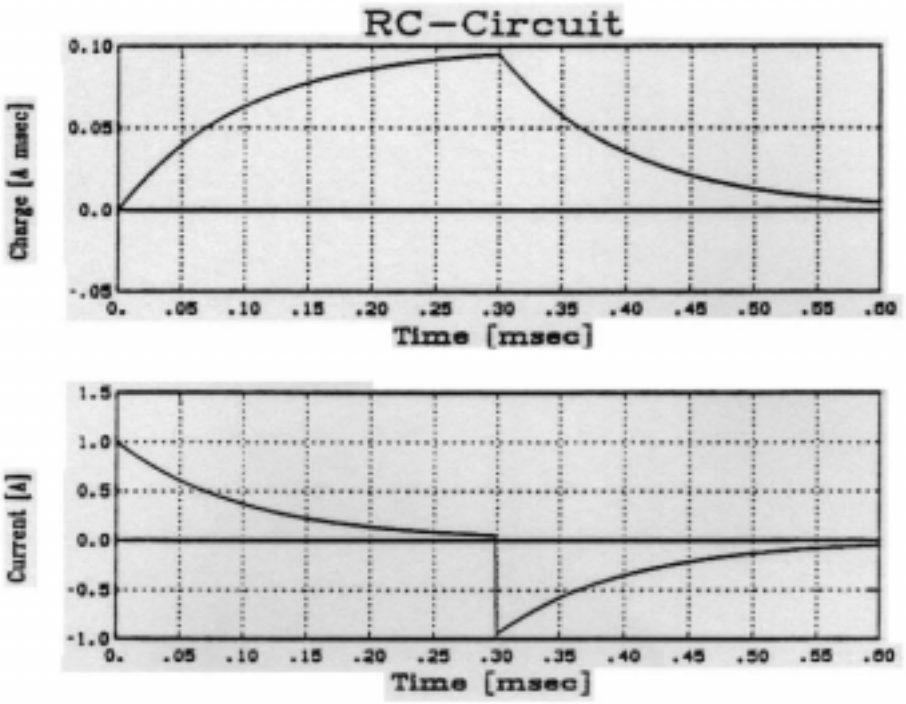

Figure 8.2. Trajectory behavior of the RC circuit

Fig.8.3 shows the relation between current and voltage in the $[i_c, u_C]$ plane which is sometimes referred to as the *phase plane* of this first order system.

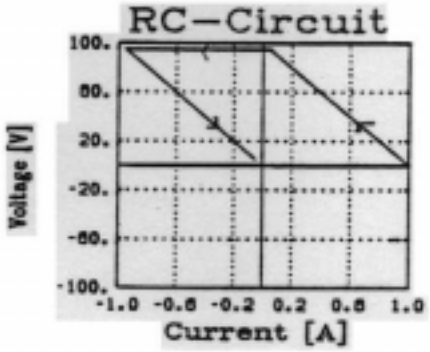

Figure 8.3. Trajectory in the phase plane

It turns out that, as long as we operate the capacitor in the first or the third quadrant of its phase plane, energy flows *into* the capacitor, otherwise it flows *out of* the capacitor.

This property actually holds not only for capacitors, but for *all* circuit elements: energy flows into the element if the effort variable and the flow variable have the same sign, and it flows out of the element otherwise.

Let us now look once more at the bond graph describing our simple passive circuit which was previously shown in Fig.7.13. This bond graph is repeated below in Fig.8.4.

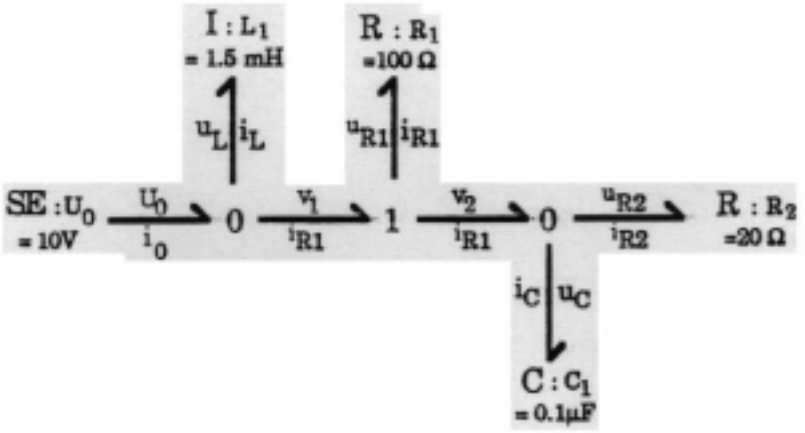

Figure 8.4. Bond graph of the passive circuit

The directions of the harpoons were, on purpose, chosen such that they indicate the *direction of energy flow*. The bond graph shows clearly how the energy is generated in the voltage source, and then spreads through the circuit and gets absorbed by the passive components. Of course, in case of an oscillation, the energy flow in the capacitor and inductor can temporarily be reversed, i.e., the capacitor and the inductor can temporarily be operated in the second and fourth quadrant of their phase planes.

What happens with the energy flow in a resistor? Obviously, since the voltage and the current in a resistor are proportional to each other, they both change their sign simultaneously, i.e., the phase plane plot of the resistor occupies the first and the third quadrant

only. Consequently, energy can flow *into* the resistor only, but never back out.

This property actually holds for *all* types of resistors, not only the linear ones. All resistors are represented in the $[f, e]$ plane (the phase plane) through (possibly non–linear) functions which are located in the first and the third quadrant of the phase plane exclusively. Fig.8.5 shows the non–linear relationship between flow and effort variables in a turbulent hydraulic "resistor".

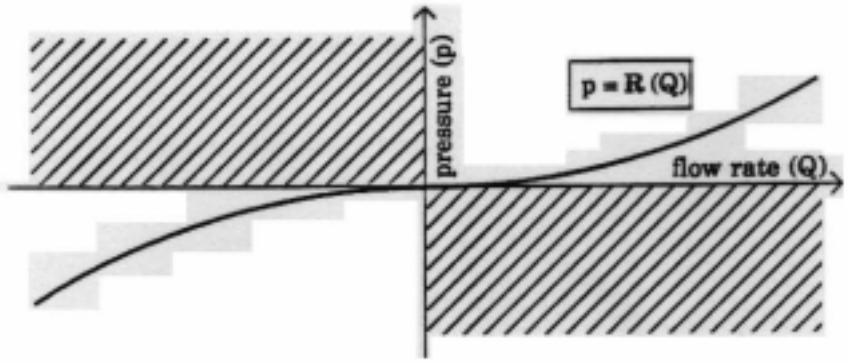

Figure 8.5. Energy dissipation in a hydraulic system

The electrical diode shown in Fig.6.5 is another example of a non–linear resistor.

How does this agree with the energy conservation law (the first law of thermodynamics) which states that, in every closed system, the total amount of energy must be preserved? This discrepancy cannot be solved within the concepts of electrical systems alone. However, we have no difficulty solving this problem if we consider the *thermic behavior* of the resistor. The resistor simply gets heated. As we see, our previously advocated resistor bond graph representation was actually incomplete. We should replace it by the enhanced bond graph representation shown in Fig.8.6 [8.16].

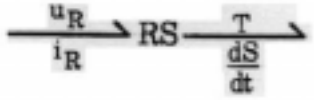

Figure 8.6. Enhanced bond graph of a resistor

Consequently, resistors are actually *two-port elements*. They have one electrical port and one thermal port. Energy can flow from the electrical side to the thermal side only, but never the other way around. On the thermal side, we use *temperature* as the effort variable, and *entropy flow* as the flow variable. In many textbooks, the entropy flow is replaced by the *heat flow*, but this is not such a good idea since the product of temperature and heat flow is not of type power. Consequently, temperature and heat flow cannot be considered *adjugate variables*. The equations governing this enhanced resistor model are as follows:

$$u_R = R(\Delta T) \cdot i_R, \quad R(\Delta T) \approx R_0 + R_1 \cdot \Delta T + R_2 \cdot \Delta T^2 \tag{8.1a}$$

$$\dot{S} = \frac{1}{T} \cdot P_{elect}, \quad P_{elect} = u_R \cdot i_R \tag{8.1b}$$

The relationship between the resistance R and the temperature T is empirical. ΔT denotes the difference between the temperature of the resistor and the temperature of its environment, R_0 is the resistive value at room temperature, and R_1 and R_2 are the first and second temperature coefficients. Eq(8.1b) simply denotes the continuity of power flow through the resistor. The causalities on either side of the RS element is arbitrary, i.e., four different causalities exist that an RS element can assume.

Since the equations for the resistor are now different from those that we used before, it has become customary among bond graphers to denote this enhanced resistor with the symbol RS rather than R. The S symbolizes the source character of this element's thermic side [8.16].

Obviously, the RS model can also be used to symbolize the heat produced in mechanical friction or any other related dissipative phenomenon.

What happens with the heat once it has been produced? Three separate physical phenomena provide mechanisms for heat transport or heat flow, namely *conduction*, *convection*, and *radiation*. Let us discuss these three phenomena one at a time.

8.2 Thermal Conduction

Heat conduction occurs naturally whenever there is a gradient in temperature. Heat flows from the warmer to the colder spot in order to approach the thermal equilibrium. The reasons for this behavior require insight into the microscopic aspects of thermodynamics, and will not be discussed here.

Let us analyze how heat is dissipated along a rod, one end of which is hot while the other is cold. The physical law that governs the thermal conduction along the rod is as follows:

$$\frac{\partial T}{\partial t} = \sigma \frac{\partial^2 T}{\partial x^2} \tag{8.2}$$

which is a *partial differential equation* (PDE) in the two independent variables t (time) and x (space). One way to approximately solve this PDE is by discretizing the space axis x while leaving the time axis t continuous. We can approximate the second derivative in space through:

$$\frac{\partial^2 T(t, x_k)}{\partial x^2} \approx \frac{T(t, x_{k+1}) - 2T(t, x_k) + T(t, x_{k-1})}{\Delta x^2} \tag{8.3}$$

where x_k denotes any particular value x, and $x_{k\pm1}$ are abbreviations for $x \pm \Delta x$. By applying this transformation, the PDE is reduced to a set of ordinary differential equations (ODE's) of the type:

$$\frac{dT_k(t)}{dt} = \frac{\sigma}{\Delta x^2}[T_{k+1}(t) - 2T_k(t) + T_{k-1}(t)], \quad k \in \{1\}, \ldots, \{n\} \tag{8.4}$$

where $T_k(t)$ denotes the temperature T at $x = x_k$ as a function of time. Now, we are back in business since we know already how to solve a set of ODE's. This technique is usually referred to as the *method of lines*.

Let us now look at one such equation, namely that for $k = i$.

$$(\frac{\Delta x^2}{\sigma}) \cdot \frac{dT_i}{dt} = T_{i+1} - 2T_i + T_{i-1} \tag{8.5}$$

Since T_i is an effort variable, this equation looks exactly like the electrical circuit equation that would result from modeling the circuit shown in Fig.8.7:

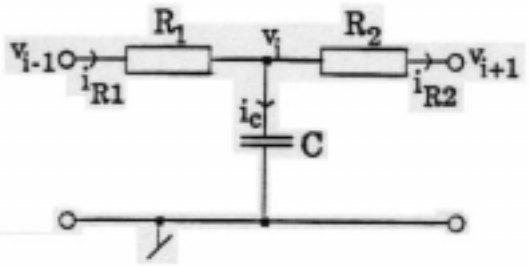

Figure 8.7. Electrical circuit diagram of an RC T–link

since:

$$C \cdot \frac{dv_i}{dt} = i_C, \quad i_C = i_{R1} - i_{R2} \tag{8.6a}$$

$$i_{R1} = \frac{v_{i-1} - v_i}{R_1}, \quad i_{R2} = \frac{v_i - v_{i+1}}{R_2} \tag{8.6b}$$

Comparison of coefficients suggests that:

$$C = \frac{\Delta x^2}{\sigma}, \quad R_1 = R_2 = 1.0 \tag{8.7}$$

However, we could also multiply the constant $\frac{\Delta x^2}{\sigma}$ to the other side of the equal sign, and then, we find that:

$$C = 1.0, \quad R_1 = R_2 = \frac{\Delta x^2}{\sigma} \tag{8.8}$$

Obviously, the analogy is not completely determined. Any combination of R 's and C 's is possible as long as:

$$R_1 \cdot C = R_2 \cdot C = \frac{\Delta x^2}{\sigma} \tag{8.9}$$

It is obvious that we can model the entire chain of ODE's through the electrical circuit analogon shown in Fig.8.8.

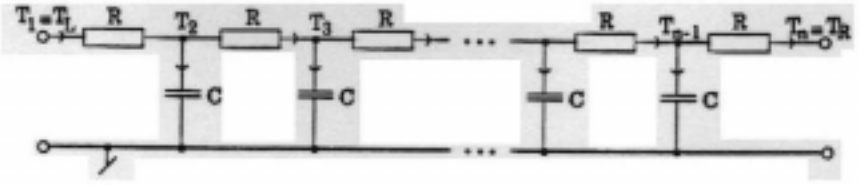

Figure 8.8. Electrical circuit analogon of a diffusion chain

A bond graph representation of this RC chain is shown in Fig.8.9

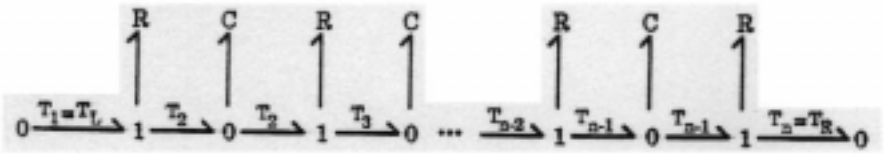

Figure 8.9. Bond graph representation of the diffusion chain

This representation would be perfectly correct if all we wanted was to model the temperature distribution along the rod as a function of time. However, our rod lives in an environment, and we must somehow model the interaction of our rod with its environment by applying appropriate boundary conditions. Here, we run into difficulties with our approach. How do we attach an entropy source to the hot end of the rod since we threw out entropy as a variable in our model altogether? Remember that, in order to represent a physical system correctly, it is insufficient to model it through a set of individual signals. The most important property of any physical system is the fact the it conserves energy, but energy was thrown out from our "model" altogether. Fig.8.10 shows the same bond graph once more, but, this time, the effort and flow variables have been appropriately named, and the causalities have been introduced. We shall find that the energy conservation requirement will present us with the missing condition to come up with a unique and correct distribution of the $\frac{\Delta x^2}{\sigma}$ factor between the R and C elements.

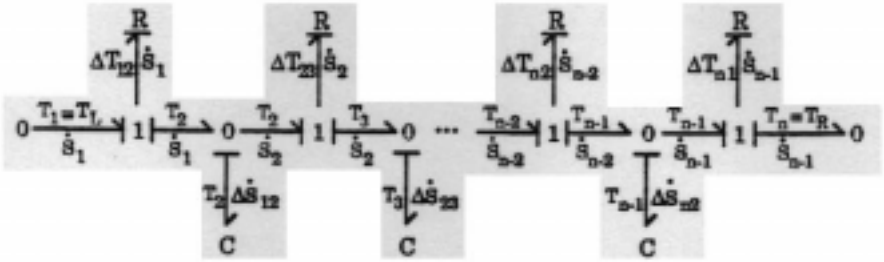

Figure 8.10. Causal bond graph of the diffusion chain

According to the first law of thermodynamics, the *total energy* E_t of a closed system is constant. The total energy is defined as the sum of the *free energy* E_f and the *thermal energy* or heat Q:

$$E_t = E_f + Q \tag{8.10}$$

The free energy is the sum of all types of energy except for the thermal one.

Eq(8.10) can be reformulated in terms of differentials. If the total *energy* of a closed system is constant, then the *power* flow into and out of the system must be zero:

$$\dot{E}_f + Q = 0.0 \tag{8.11}$$

We shall define the *entropy flow* $\dot{S}$ of a body as its heat flow $\dot{Q}$ divided by its temperature:

$$\dot{S} = \frac{\dot{Q}}{T} \tag{8.12}$$

Notice that our definition of *entropy flow* is not totally in accordance with the usual thermodynamic definition of *entropy*. However, it is commonly used among bond graphers, and it is useful for our purpose.

The capacity of a body to transport heat in a dissipative manner can be described by the equation:

$$\Delta T = \theta \cdot \dot{Q} = (\theta \cdot T) \cdot \dot{S} \tag{8.13}$$

where θ is the *thermal resistance* of the body. This looks very much like Ohm's law, and we can thus also write:

$$\Delta T = R \cdot \dot{S}, \quad R = \theta \cdot T \tag{8.14}$$

Here, the reason becomes evident why many textbooks prefer to use the heat flow $\dot{Q}$ rather than the entropy flow $\dot{S}$ as the bond graph's flow variable: using heat flow, the resistor assumes a constant value, while using entropy flow, the resistor is modulated (multiplied) with the effort variable T. However, using DYMOLA as a modeling tool, this does not cause any problem and is therefore a small price to pay.

For a rod of length ℓ and cross-section A, we find that the thermal resistance can be written as:

$$\theta = (\frac{1}{\lambda}) \cdot (\frac{\ell}{A}) \tag{8.15}$$

where λ denotes the *specific thermal conductance* of the material. Again, this looks exactly the same as the corresponding equation for a rod–shaped electrical resistor. Since we have cut our rod into small segments of length Δx, we replace eq(8.15) by:

$$R = \theta \cdot T = \frac{\Delta x \cdot T}{\lambda \cdot A} \tag{8.16}$$

The capacity of a body to store heat is expressed through the equation:

$$\Delta \dot{Q} = \gamma \frac{dT}{dt} \tag{8.17}$$

where γ denotes the *thermal capacitance* of the body. This equation can also be written as:

$$\Delta \dot{S} = C \frac{dT}{dt}, \quad C = \frac{\gamma}{T} \tag{8.18}$$

Notice that the terms "thermal resistance" and "thermal capacitance" were traditionally introduced for the relationship between temperature and heat, and not for the relationship between temperature and entropy which is truly regrettable. The thermal capacitance of a body can be written as:

$$\gamma = c \cdot m \tag{8.19}$$

where m is the mass of the body, and c is the *specific thermal capacitance* of the material. The mass can further be written as the product of density ρ and volume V:

$$m = \rho \cdot V \tag{8.20}$$

and, for our rod segment:

$$V = A \cdot \Delta x \tag{8.21}$$

and thus:

$$C = \frac{\gamma}{T} = \frac{c \cdot \rho \cdot A \cdot \Delta x}{T} \tag{8.22}$$

Consequently, we can determine the time constant of our diffusion equation to be:

$$R \cdot C = \theta \cdot \gamma = \frac{c \cdot \rho}{\lambda} \Delta x^2 \tag{8.23}$$

or:

$$\sigma = \frac{\lambda}{c \cdot \rho} \tag{8.24}$$

At this point, we know how to dimension both the resistive and capacitive elements in our bond graph in order to reflect the physicality of our equations.

The bond graph shown in Fig.8.10 exhibits still one small problem. As in the electrical case, we seem to have resistances that dissipate heat, and thereby "lose" energy. Well, the energy is not lost, it is simply reintroduced right away at the next node as shown in Fig.8.11.

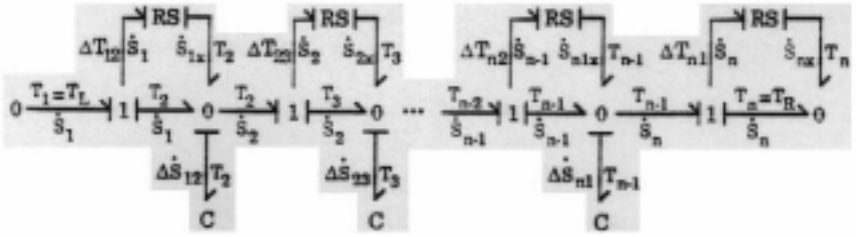

Figure 8.11. Corrected causal bond graph for the diffusion chain

Therefore, the i^{th} computational cell of our diffusion chain can be described through the following set of equations:

$$\frac{dT_i}{dt} = \frac{1}{C}\Delta\dot{S}_i \tag{8.25a}$$

$$\Delta T_i = T_{i-1} - T_i \tag{8.25b}$$

$$\dot{S}_{i-1} = \frac{1}{R}\Delta T_i \tag{8.25c}$$

$$\dot{S}_{ix} = \dot{S}_{i-1}\frac{\Delta T_i}{T_i} \tag{8.25d}$$

$$\Delta\dot{S}_i = \dot{S}_{i-1} + \dot{S}_{ix} - \dot{S}_i \tag{8.25e}$$

where T_{i-1} is being determined by the computational cell to the left, while $\dot{S}_i$ is being determined by the computational cell to the right.

Notice that our modified bond graph is no longer exactly equivalent to the electrical circuit analogon. While the electrical circuit is able to represent the temperature distribution correctly, it fails to also represent the energy flow adequately.

The bond graph shown in Fig.8.11 is not symmetrical, i.e., it favors heat flow from the left to the right. This is, of course just an approximation to what is really going on in the distributed parameter system. We could as well have decided to reintroduce the lost heat one element further left instead of one element further right, or we could have split the *RS* element into two equal parts, one turning left, and the other turning right. However, the last alternative is not such a desirable choice since it introduces algebraic loops as can be easily verified since we have now some freedom in assigning the causalities at the *RS* elements as shown in Fig.8.12.

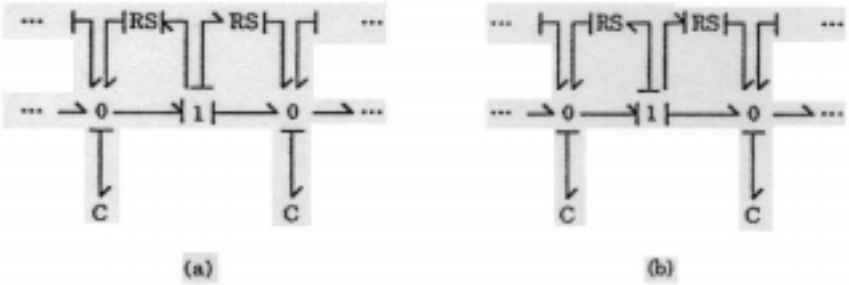

Figure 8.12. Causality choices in symmetric causal bond graph

It is usually a good idea to bias the *RS* elements away from the hot and towards the cold end of the rod.

How about the boundary conditions? Let me first assume that the "rod" being modeled is the electrical resistor itself. In that case, we must cut our electrical resistor into small resistors of length Δx which are connected in series. Each one of these resistors contains a small entropy source which introduces entropy into the thermal network as shown in Fig.8.13.

A series connection of resistors is represented in the bond graph as a set of resistors all attached to the same 1–junction which, for topological reasons, has been split into several "1–junctions". However, the harpoons in between those junctions were left out to symbolize that these represent, in reality, one and the same junction. Since the capacitances determine the temperatures at each 0–junction, the thermal input at each of these junctions must assume the causality of an entropy source rather than that of a temperature source. Had we decided to introduce the external energy at the 1–junctions instead of at the 0–junctions, we would have introduced algebraic loops as can be easily verified. Also, it is important to introduce the electrical power in the form of a current source rather than in the form of

a voltage source in order to avoid the creation of another algebraic loop.

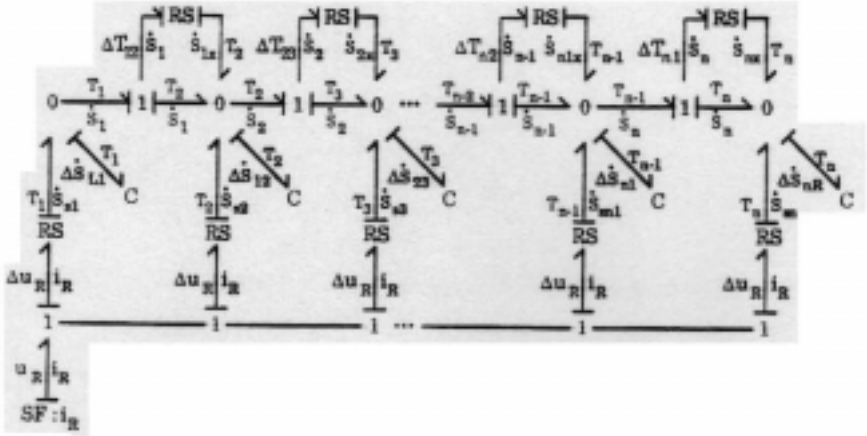

Figure 8.13. Causal bond graph for the heated rod resistor

If the resistor represents a source of heat or temperature at one end of a narrow and radially well insulated thin air channel (say, my meerschaum pipe), then the entropy source is simply introduced at the "hot" end of the "rod" as shown in Fig.8.14.

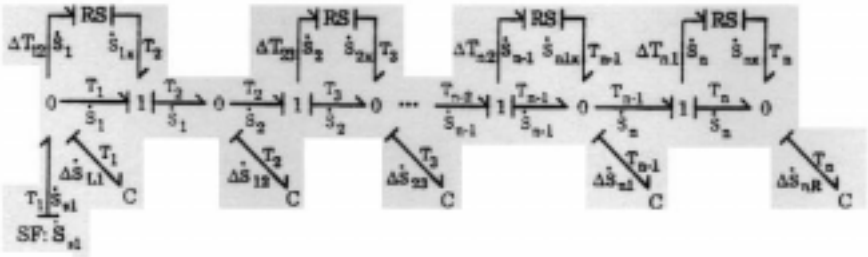

Figure 8.14. Causal bond graph for the heated air channel

If we decide to introduce the external energy at the nearest 0–junction, we must use a heat source in order to avoid a structural singularity. Had we decided to introduce the external energy at the nearest 1–junction instead, we could have used either type of energy source. Distributed parameter systems often provide us with some flexibility which can be exploited in avoiding algebraic loops and/or structural singularities.

The concepts shown so far can easily be extended to multidimensional heat flow problems. In this case, the heat equation is modified as follows:

$$\frac{\partial T}{\partial t} = \sigma \cdot \nabla^2 T \qquad (8.2^{alt})$$

where ∇^2, for the three–dimensional case, is the Laplacian operator:

$$\nabla^2 = \frac{\partial^2}{\partial x^2} + \frac{\partial^2}{\partial y^2} + \frac{\partial^2}{\partial z^2} \qquad (8.26)$$

Let us discuss the two–dimensional case. In order to apply the method of lines approach to an n–dimensional problem, we always discretize $n-1$ independent variables, and leave one variable (usually the time t) continuous. Consequently:

$$\nabla^2 T(t, x_k, y_k) \approx \frac{T(t, x_{k+1}, y_k) - 2T(t, x_k, y_k) + T(t, x_{k-1}, y_k)}{\Delta x^2} + \frac{T(t, x_k, y_{k+1}) - 2T(t, x_k, y_k) + T(t, x_k, y_{k-1})}{\Delta y^2} \qquad (8.27)$$

which leads to the electrical circuit analogon shown in Fig.8.15 as can be easily verified.

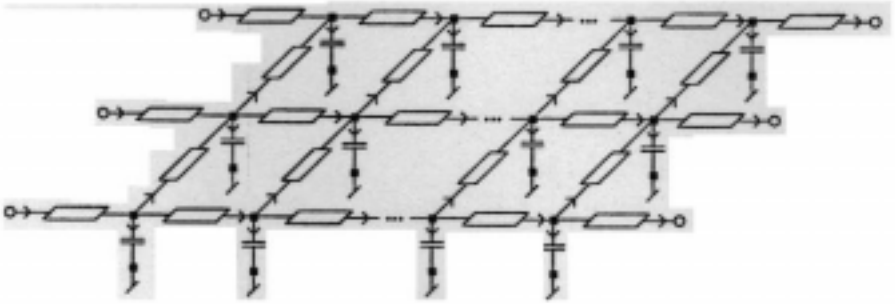

Figure 8.15. Electrical analogon for a two–dimensional diffusion

Such electrical circuit analogies for the representation of distributed parameter systems are sometimes referred to as *Beuken models* [8.6].

I refrain from presenting here the correct bond graph for the two–dimensional case since the graph would be rather busy. However, generating such a bond graph is not conceptually difficult, just a little more work.

At this point, one may jump to the conclusion that the bond graph representation is necessarily more complicated than the "equivalent" electrical analogon, but this is not really the case. Remember that the bond graph is not simply another representation scheme for the same thing. It provides *more information* than the electrical circuit diagram since it represents the topological as well as the computational structure of the system, and moreover, since the electrical circuit diagram is even *incorrect* with respect to the representation of the energy flow in the system.

Let us model a computational cell of a three–dimensional heat flow model in DYMOLA. The DYMOLA equivalent of the *RS* element is presented below.

```
model type RS
  cut A(e1/f1) B(e2/ - f2)
  main cut C[A B]
  main path P < A - B >
  parameter R = 1.0
  R * f1 = e1
  e1 * f1 = e2 * f2
end
```

However, *RS* elements with a thermal primary side must be modeled using a modulated *RS* element as shown below, since the resistance is multiplied with the temperature (i.e., the effort variable).

```
model type mRS
  cut A(e1/f1) B(e2/ - f2)
  main cut C[A B]
  main path P < A - B >
  parameter theta = 1.0
  R = theta * e2
  R * f1 = e1
  e1 * f1 = e2 * f2
end
```

Notice that the modulation uses the secondary effort e_2 and not the primary effort e_1, since e_2 denotes an absolute temperature whereas e_1 is a temperature difference.

Similarly, thermal capacitances must also be "modulated", since the capacitor must be divided by the temperature.

```
model type mC
  cut A(e/f)
  parameter gamma = 1.0
  C = gamma/e
  C*der(e) = f
end
```

Notice that the "modulation" of a capacitance is a rather dubious undertaking. How do we ensure that the "modulated" capacitance

is still an energy storage element, and does not suddenly start to dissipate energy? This problem requires some further contemplation.

The energy stored in a capacitor (or inductor) is the integrated power that flows into that capacitor (or inductor), thus:

$$E(t) = \int_0^t P(\tau)d\tau = \int_0^t e(\tau) \cdot f(\tau)d\tau \tag{8.28}$$

whereby the energy for $t = 0.0$ has arbitrarily been normalized to zero. Using the formula for the general displacement (the charge) of the capacitor:

$$q(t) = \int_0^t f(\tau)d\tau \tag{8.29}$$

we can write:

$$E(t) = \int_0^t e(\tau) \cdot \dot{q}(\tau)d\tau = \int_0^q e(q)dq \tag{8.30}$$

Thus, in order for an element to behave like a capacitor, the effort e must be expressible as a (possibly non–linear) function of q:

$$e_C = \Phi_C(q_C) \tag{8.31}$$

Similarly, we can use the formula for the generalized momentum (the flux) of an inductor:

$$p(t) = \int_0^t e(\tau)d\tau \tag{8.32}$$

Therefore, in order for an element to behave like an inductor, the flow f must be expressible as a (possibly non–linear) function of p:

$$f_I = \Phi_I(p_I) \tag{8.33}$$

Let us check whether our "modulated" capacitance satisfies eq(8.31). We know that:

$$f_C(t) = C \cdot \dot{e}_C(t) = \frac{\gamma}{e_C(t)} \cdot \dot{e}_C(t) \tag{8.34}$$

and therefore:

$$q_C(t) = \int_0^t f_C(\tau)d\tau = \gamma \int_0^t \frac{\dot{e}_C(\tau)}{e_C(\tau)}d\tau = \gamma \cdot \log(e_C) \qquad (8.35)$$

The capacitive charge q_C is indeed a non–linear function of the effort e_C, and the capacitive nature of our "modulated" capacitance has thus been verified.

Let us return to our heat flow problem now. We want to assume that each cell consists of one "modulated" capacitor, and three modulated resistors, namely the one to its left, the one to its front, and the one below as shown in Fig.8.16. Remember that, for DYMOLA modeling, bond graphs must be enhanced to avoid the necessity to attach any elements to 1–junctions.

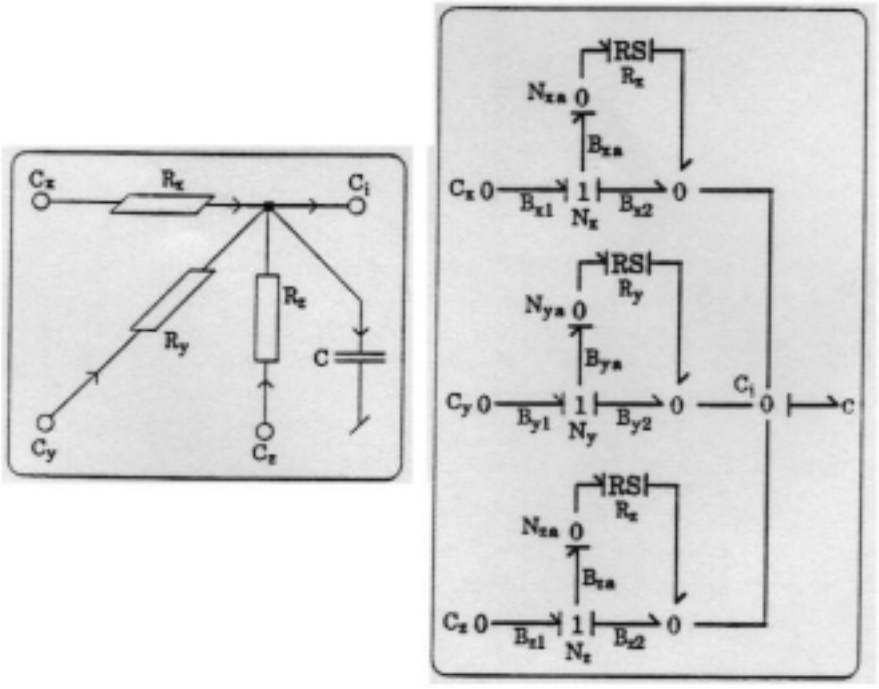

Figure 8.16. Three–dimensional diffusion cell

The following DYMOLA model describes a three–dimensional diffusion cell:

```
model type c3d

  submodel (mRS) Rz, Ry, Rz
  submodel (mC) C(lc e = 298.0)
  submodel (bond) Bz1, Bz2, Bza, By1, By2, Bya, Bz1, Bz2, Bza
  node Nz, Nza, Ny, Nya, Nz, Nza

  cut Cz(ez/fz), Cy(ey/fy), Cz(ez/fz), Ci(ei/ - fi)
  path Pz < Cz - Ci >, Py < Cy - Ci >, Pz < Cz - Ci >

  connect Bz1 from Cz  to Nz
  connect By1 from Cy  to Ny
  connect Bz1 from Cz  to Nz
  connect Bz2 from Nz  to Ci
  connect By2 from Ny  to Ci
  connect Bz2 from Nz  to Ci
  connect Bza from Nz  to Nza
  connect Bya from Ny  to Nya
  connect Bza from Nz  to Nza
  connect Rz  from Nza to Ci
  connect Ry  from Nya to Ci
  connect Rz  from Nza to Ci
  connect C   at   Ci

end
```

Notice one additional new concept: While invoking the submodel C of model type mC, we assigned an *initial condition* of $T = 298.0°K$ to the integrator inside the mC model.

Now, we can create a diffusion model that contains as many computational cells as we need, say the 27 $c3d$ cells $C111, \ldots C333$, three in each direction. These cells are then best connected through their paths with statements such as:

```
connect (Pz) C111 - C211 - C311, C112 - C212 - C312
connect (Py) C111 - C121 - C131, C112 - C122 - C132
connect (Pz) C111 - C112 - C113, C121 - C122 - C123
```

Altogether, 27 such connections will be needed. Then, we must attach additional capacitors to each of the left–most, front–most, and bottom–most $c3d$ cells, and set the entropy flow equal to zero at each of the right–most, back–most, and top–most cells. Finally, we may attach entropy sources to any of the cells as desired for the purpose of modeling thermal input.

8.3 Thermal Convection

So far, we have discussed only one mechanism of heat transfer, namely *diffusion*, i.e., heat transfer that is caused by the microscopic motion of individual particles. However, heat is attached to *matter*, and a second form of heat transfer is by means of moving matter around on a macroscopic scale. Obviously, the heat stored in any moving piece of matter is transferred together with that matter. This physical phenomenon is called *convection*. It describes the transfer of heat as a result of macroscopic rather than microscopic movement.

Convection can occur autonomously. If we heat the floor of a room, the surrounding air expands, and thereby its density is being reduced. Consequently, the hot air moves upward toward the ceiling, and is replaced by colder air that moves down toward the floor. This is a typical example of a convective phenomenon.

Convection can also be artificially induced. In a room which is heated through a warm water radiator, the convection can be increased by installing a fan that blows at the radiator. This fan will increase the air circulation in the vicinity of the radiator, and thereby increases the convection.

Let us model convection mechanisms in a solar heating system. Water is contained in a pipe which connects the water heater with the solar collector. At the solar collector, the water is heated by the sun (mostly through thermal radiation). The sun also feeds a solar battery which drives a small pump that circulates the water from the water heater to the collector and back, i.e., the mechanism of transferring the heat from the solar collector to the water heater is primarily convective.

Let us assume that the pipe is free of air, and that the water in the pipe is totally incompressible. Under this assumption, water will flow through the entire pipe with a constant velocity v_w as soon as the solar battery turns on the pump. Heat will thereby be transferred from one computational cell to the next.

Let q denote the hydraulic flow rate expressed in $m^3\ sec^{-1}$. The volume of water in one computational cell is $V = A \cdot \Delta x$. Therefore, the amount of entropy that leaves the i^{th} computational cell per time unit to the right is:

$$\dot{S}_{i\ out} = \Delta S_i \cdot \frac{q}{V} \tag{8.36}$$

which can also be written as:

$$\dot{S}_{i\ out} = (C \cdot \frac{q}{V}) \cdot T_i \tag{8.37}$$

In the same time unit, a similar amount of heat is transferred into the cell from its left neighbor:

$$\dot{S}_{i\ in} = (C \cdot \frac{q}{V}) \cdot T_{i-1} \tag{8.38}$$

These two equations can be combined into:

$$\dot{S}_{i\ conv} = G_{conv} \cdot \Delta T_i, \quad G_{conv} = C \cdot \frac{q}{V} \tag{8.39}$$

Consequently, the effect of the convection is simply a second *convective resistance* which is connected in parallel with the *conductive resistance*, i.e., convection simply increases the thermal conductivity.

Obviously, the above equations contain a number of implicit simplifications. In reality, we ought to consider the friction between the liquid and the wall, and the friction within the liquid. By doing so, we would see that the liquid flows faster at the center of the pipe, and slower in the vicinity of the wall. The hydraulic friction is again a dissipative process which produces more heat and therefore should result in additional small entropy sources applied to the thermal model.

If we let go of the assumption of incompressibility, for example, if we model a gas flowing through the pipe rather than a liquid, the situation becomes much more complicated. Now, we need to model the pneumatic process in addition to the thermal process. The pneumatic process will generate a time– and space–dependent flow rate $q(t, x)$ which can be used to modulate the convective resistance of the thermal model. The fluid dynamics model would also have to provide equations for the pneumatic dissipation which could then be used to drive additional RS elements which bridge over from the pneumatic to the thermal subsystem. However, we shall not pursue this avenue any further.

8.4 Thermal Radiation

The third mechanism of heat transport is through thermal radiation, i.e., the emission/absorption of light. In order to fully understand the rationale behind thermal radiation, we would again need to look

into the microscopic aspects of thermodynamics. However, we can analyze the macroscopic effects of thermal radiation using the law of Stefan–Boltzmann which states that the emitted/absorbed radiation of a body is proportional to the fourth power of its temperature:

$$\mathcal{R} = \sigma \cdot T^4 \tag{8.40}$$

where σ is different from the σ that we met previously in thermal conduction. σ here denotes the capability to emit and/or absorb light which depends on the body's *color*. Black bodies emit/absorb much more strongly than white bodies — that is why there aren't so many dark painted cars here in Arizona. $\mathcal{R}$ is the emitted/absorbed power per unit surface. Consequently, this equation can be rewritten as:

$$\dot{Q} = \sigma \cdot A \cdot T^4 \tag{8.41}$$

where A denotes the emitting surface, or, in terms of the emitted/absorbed entropy:

$$\dot{S} = \sigma \cdot A \cdot T^3 \tag{8.42}$$

which is the version of the Stefan–Boltzmann law that I prefer. Also the radiation phenomenon is clearly dissipative. It can be described by yet another (non–linear) R or RS element where:

$$R = \frac{T}{\dot{S}} = \frac{1}{\sigma \cdot A \cdot T^3} \tag{8.43}$$

which is again a modulated resistor. As with all other dissipative elements, the causality of this element is not predetermined. Emitted radiation usually uses temperature as a cause while absorbed radiation usually assumes the causality of an entropy source. Therefore, RS elements describing radiation are usually located between two 0–junctions as shown in Fig.8.17:

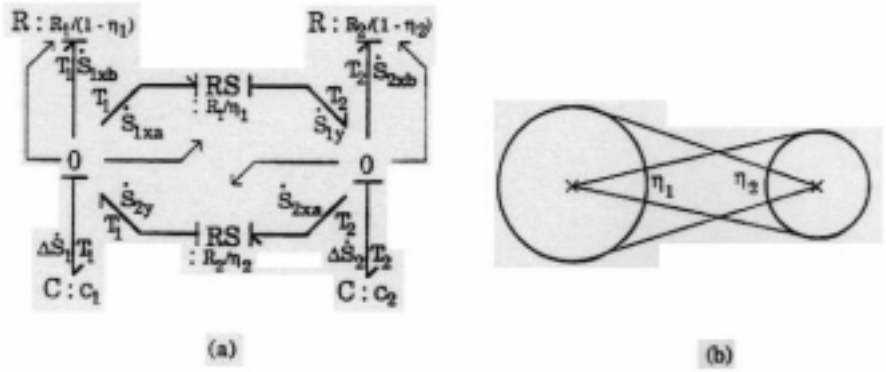

Figure 8.17. Power exchange between two bodies through radiation

η_1 denotes the percentage of the surface of the first body that radiates toward the second body, and η_2 denotes the percentage of the surface of the second body that radiates toward the first. This is shown in Fig.8.17b. The thin full arrows are *signal paths*. They symbolize the *temperature modulation* of the dissipative elements. This bond graph leads to the following set of equations:

$$\dot{S}_{1xa} = \frac{1}{R_1/\eta_1} \cdot T_1 = \eta_1 \cdot \frac{1}{R_1} \cdot T_1 \tag{8.44a}$$

$$\dot{S}_{1xb} = (1-\eta_1) \cdot \frac{1}{R_1} \cdot T_1 \tag{8.44b}$$

$$\dot{S}_{1y} = \frac{T_1}{T_2} \cdot \dot{S}_{1xa} \tag{8.44c}$$

$$\dot{S}_{2xa} = \eta_2 \cdot \frac{1}{R_2} \cdot T_2 \tag{8.44d}$$

$$\dot{S}_{2xb} = (1-\eta_2) \cdot \frac{1}{R_2} \cdot T_2 \tag{8.44e}$$

$$\dot{S}_{2y} = \frac{T_2}{T_1} \cdot \dot{S}_{2xa} \tag{8.44f}$$

$$R_1 = \frac{1}{\sigma_1 \cdot A_1 \cdot T_1^2} \tag{8.44g}$$

$$R_2 = \frac{1}{\sigma_2 \cdot A_2 \cdot T_2^2} \tag{8.44h}$$

8.5 Thermal Inertance: The Missing Link

A strange discrepancy may be noticed in Table 7.1. The table suggests that thermodynamic systems don't possess a generalized momentum. Since the generalized momentum can always be expressed as the product of inertance and flow, this is equivalent to saying that thermodynamic systems don't possess inertance. Indeed, none of the bond graphs shown in this chapter exhibits any inertances.

It has been shown that the existence of a thermic inertance would be in contradiction with the second law of thermodynamics which states that, in a closed system, the total entropy can never decrease [8.1]:

$$\dot{S}_{total} \geq 0 \tag{8.45}$$

In *reversible thermodynamics*, according to eq(8.17), the total entropy is always kept in balance, while in *irreversible thermodynamics* [8.13,8.18], according to eq(8.13), the total entropy always grows, unless the RS element has two thermic ports, in which case the entropy stays in balance. One of the consequences of the second law is the fact that spontaneous heat flow can never occur from a point of lower temperature to a point of higher temperature. (A cold body can radiate heat to a hot body, but the radiation in reverse direction will always over–compensate, i.e., in the balance, heat still flows from the hot to the cold body.)

Now, let us assume that we found a thermic inertance. Its state equation would be:

$$\Delta T = I \cdot \frac{d\dot{S}}{dt} \tag{8.46}$$

i.e., the thermic inertance can be used as a storage element for entropy flow which indicates that a constant entropy flow may exist even for ΔT being equal to zero. This is clearly in contradiction with the second law, and thus, thermic inertances indeed do not exist.

Is this statement in contradiction with the observed heat wave (or: "second sound" wave) in superfluid Helium (Helium–II) [8.10,8.11,

8.12]? It is correct that a linear system with *constant* R and C coefficients can never oscillate. However, this statement is no longer true when we allow the R and C parameters to be modulated by other variables. One possible explanation for the second sound wave is through *convection*. If the hydraulic subsystem produces an oscillating flow rate q, then this flow rate will modulate the convective resistance in such a way that a heat wave can indeed occur. Also, the thermal capacitance is strongly non–linear in the vicinity of the so–called λ–point, i.e., the point of transition between liquid Helium–I and superfluid Helium–II. A nice research topic would be to formulate the so–called two–fluid theory in terms of the bond graph methodology, and thereby come up with a simulation model that reproduces the observed second sound wave while conserving both energy and mass in the system.

8.6 Irreversible Thermodynamics

One of the properties of state–space models is the fact that they allow us to "reverse time" (at least in a mathematical sense) in a trivial manner. Let me explain this concept. We want to discuss the general non–linear state–space model:

$$\frac{d\mathbf{x}(t)}{dt} = \mathbf{f}(\mathbf{x}(t), \mathbf{u}(t), t) \tag{8.47}$$

which we can simulate forward in time:

$$t : t_0 \longrightarrow t_f, \quad t_f > t_0$$

Now, we wish to "reverse time", and simulate the system backward in time:

$$\tau : t_f \longrightarrow t_0, \quad t_0 < t_f$$

such that the final state of the reversed model is the same as the initial state of the original model. Obviously, this can be achieved with the simple transformation:

$$\tau = t_0 + t_f - t \tag{8.48}$$

and therefore:

$$\frac{dt}{d\tau} = -1 \tag{8.49}$$

Consequently, we can rewrite our state–space model in the new independent variable τ as:

$$\frac{d\mathbf{x}(\tau)}{d\tau} = \frac{d\mathbf{x}(t)}{dt} \cdot \frac{dt}{d\tau} = -\mathbf{f}(\mathbf{x}(\tau), \mathbf{u}(\tau), \tau) \tag{8.50}$$

In other words, by simply placing an inverter at the input of every integrator in the state–space model, we can reverse the time–behavior of any state–space model.

Let us demonstrate this concept by means of a second order autonomous time–invariant system, the famous Van–der–Pol oscillator, in which the time reversal can be easily visualized. This example will, in addition, teach us some basic properties of trajectory behavior of state–space models.

The Van–der–Pol oscillator is described by the following second order differential equation:

$$\ddot{x} - \mu(1 - x^2)\dot{x} + x = 0 \tag{8.51}$$

By choosing the outputs of the two integrators as our two state variables:

$$x_1 = x, \quad x_2 = \dot{x}$$

we obtain the state–space model:

$$\dot{x}_1 = x_2 \tag{8.52a}$$
$$\dot{x}_2 = \mu(1 - x_1^2)x_2 - x_1 \tag{8.52b}$$

We coded this model in ACSL (another trivial exercise), and ran six different simulations with various sets of initial conditions for the two state variables x_1 and x_2. Fig.8.18 shows the results of this simulation.

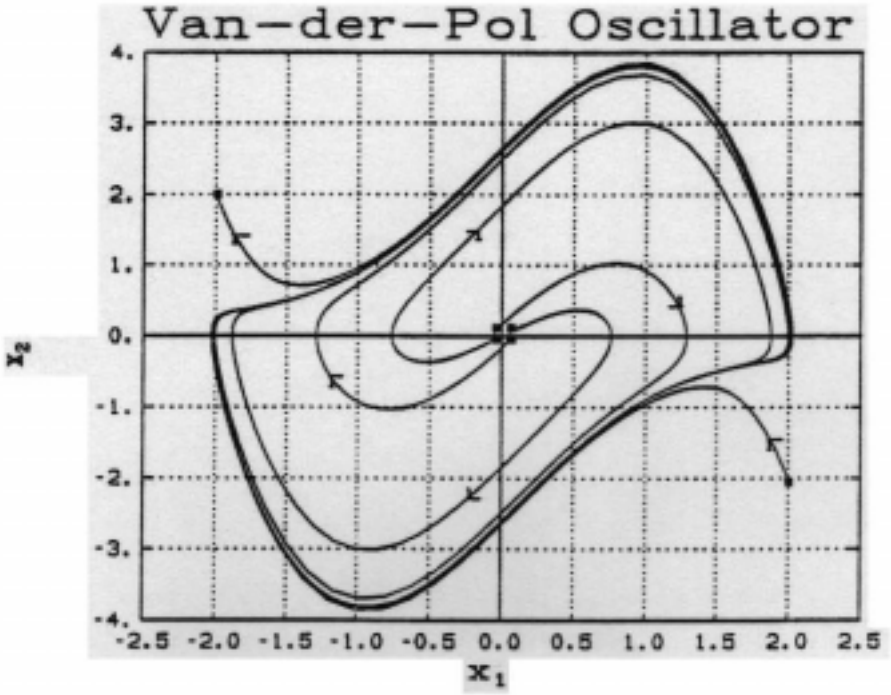

Figure 8.18. Trajectory behavior of the Van–der–Pol oscillator

Fig.8.18 shows a phase–portrait of x_2 plotted as a function of x_1. Four of the initial conditions were chosen very close to the origin which is an unstable singularity. It becomes obvious that the solution is extremely sensitive to the initial condition when the initial condition is chosen close to the origin. The other two initial conditions were chosen far away from the origin. It turns out that a stable limit cycle exists which attracts all trajectories emanating from any point in the phase plane except for the origin itself.

We then applied the above described time reversal algorithm which leads us to the following set of equations:

$$\dot{x}_1 = -x_2 \tag{8.53a}$$

$$\dot{x}_2 = -\mu(1 - x_1^2)x_2 + x_1 \tag{8.53b}$$

which we again simulated using four different initial conditions as shown in Fig.8.19. The former limit cycle is here not part of any

trajectory. It was simply copied over from Fig.8.18 for an easier comparison between the two figures.

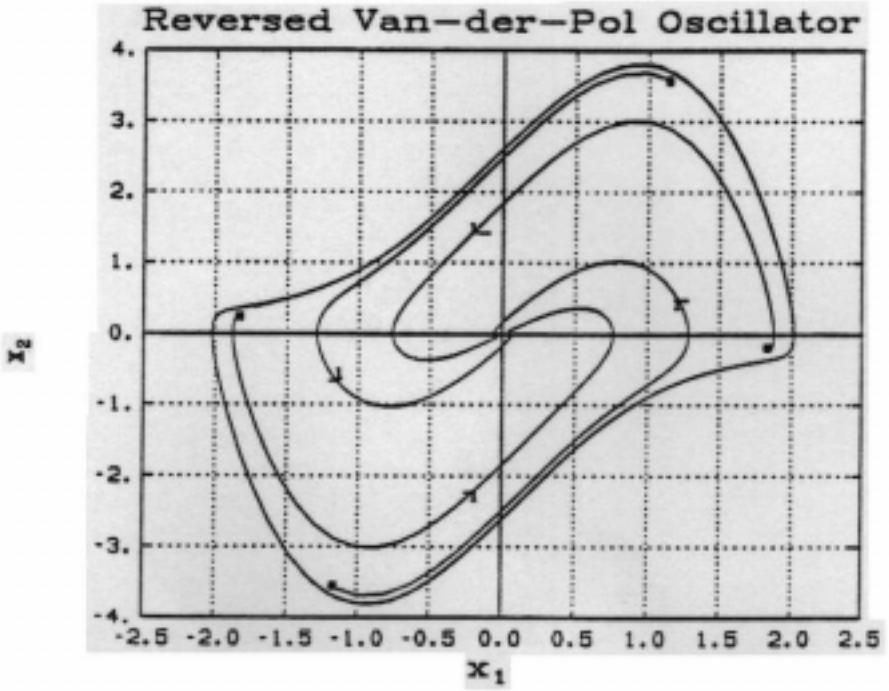

Figure 8.19. Trajectory behavior of the reversed Van–der–Pol equation

The formerly unstable singularity at the origin has now become a stable singularity, a so–called *attractor*. The formerly stable limit cycle has turned into an unstable limit cycle. Trajectories emanating from anywhere inside the limit cycle are attracted by the singularity at the origin, whereas trajectories emanating from anywhere outside the limit cycle escape to infinity. The limit cycle has thus become a border line between two domains, the region of stability (the domain of attraction) of the singularity at the origin, and the unstable domain encompassing it.

It can be observed that, in the phase plane, the two sets of time–trajectories look exactly the same, only the direction of the arrows has been reversed.

We also ran the following experiment. Starting from the initial condition $[x_1, x_2] = [0.1, 0.1]$, we simulated the original Van–der–Pol

equation over 2 *sec*. Thereafter, we reversed the sign of the inputs to the two integrators, and continued to simulate the system for another 2 *sec*. This ACSL program is a little more interesting, therefore, let me write down the code:

```
Program oscillator
  Initial
    Constant tmx = 4.0, x10 = 0.1, x20 = 0.1, c = 1.0
    Cinterval cint = 0.05
    schedule revers .at. 2.0
    End $ "of Initial"
  Dynamic
    Derivative
      x1d = x2
      x2d = 2.0 * (1.0 - x1 * x1) * x2 - x1
      x1  = INTEG(c * x1d, x10)
      x2  = INTEG(c * x2d, x20)
    End $ "of Derivative"
    Discrete revers
      c = -1.0
    End $ "of Discrete revers"
    Termt(t.ge.tmx)
  End $ "of Dynamic"
End $ "of Program"
```

The time–event *revers* was used to model the discrete event of switching between the two modes of the simulation. Fig.8.20 shows the results of this simulation. The final values of the two state variables were again $[x_1, x_2] = [0.1, 0.1]$, correct up to eight digits, i.e., we have successfully reversed the model to the original initial conditions.

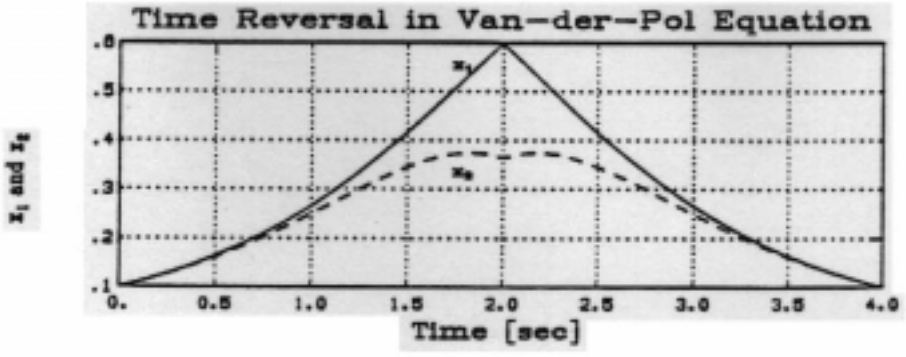

Figure 8.20. Time reversal for the Van–der–Pol equation

However, let us see what this seeming "time reversal" really means. Fig.8.21 shows the plot of the two state derivatives $\dot{x}_1$ and $\dot{x}_2$ over time.

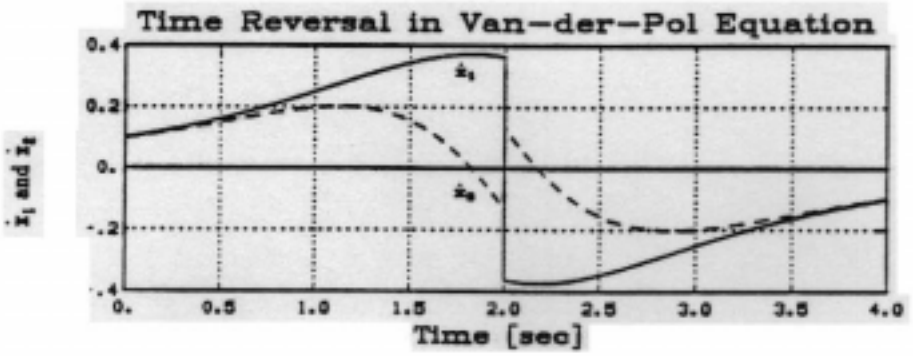

Figure 8.21. Time reversal for the Van-der-Pol equation

Obviously, these two variables were not properly reversed. "Time reversal", in a mathematical sense, means the reversal of all *state variables* in the model. However, the *state derivatives* are not reversed; they change their sign. This can be easily seen from the "reversed" state-space model.

In an electrical circuit, the most commonly used state variables are the currents through the inductances, and the voltages across capacitors. Consequently, in a time reversal, those will remain the same. However, the voltages across inductances and the currents through capacitors will change their sign. Therefore, time reversal is an illusion.

Let us now repeat the above experiment, but, this time, we shall simulate the original system forward in time over 20 *sec* before we apply time reversal.

The final state after 40 *sec* is now $[x_1, x_2] = [1.59 \times 10^{-5}, 1.59 \times 10^{-5}]$, i.e., completely wrong. Fig.8.22 shows the time trajectories of the two state variables.

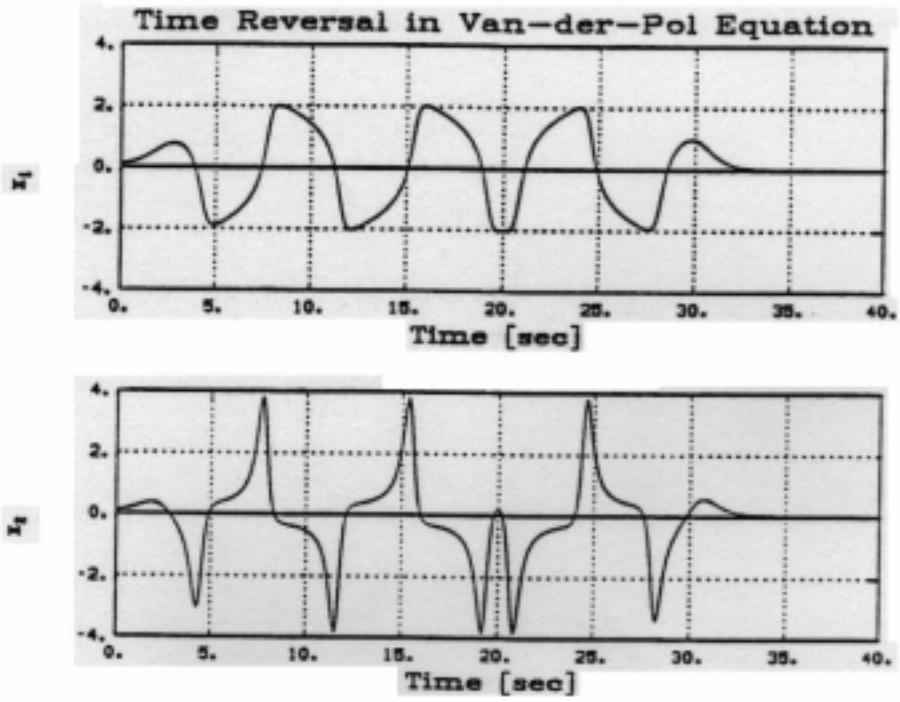

Figure 8.22. "Time reversal" for the Van–der–Pol equation

Shortly after time 20 *sec*, the time reversal seems to work just fine, but thereafter, around time 28 *sec*, the trajectories suddenly deviate from their expected paths, and skip one whole oscillatory cycle. What is the reason for this unexpected behavior?

The Van–der–Pol oscillator exhibits two types of *singularities*. The origin, i.e. the point $[x_1, x_2] = [0, 0]$, is an *unstable equilibrium point*. If we start at the origin, x_1 and x_2 will stay at the origin forever, i.e., the trajectory consists of a single point. However, the smallest disturbance away from the origin in any direction will make the trajectory move away from the origin, and approach the second singularity which is a *stable limit cycle*.

It becomes immediately evident that the sensitivity of the trajectory to the initial condition grows larger and larger, the closer to the unstable singularity the initial condition is chosen. At the singularity itself, the sensitivity is infinite. This can be easily seen from Fig.8.18 where four of the initial conditions were chosen very close to

the origin, and the resulting trajectories were rather different. For all practical purposes, we can say that the trajectory behavior is *non-deterministic* if the initial condition is chosen in the vicinity of the unstable singularity.

If we reverse the time, the previously unstable equilibrium point turns into a stable equilibrium point (an attractor), whereas the previously stable limit cycle turns into an unstable limit cycle, i.e., the region inside the unstable limit cycle is now the *domain of attraction* of the stable equilibrium point. This provides us actually with an excellent technique to determine the domain of attraction of any stable equilibrium point of a second order system. We simply reverse time and simulate the system until the trajectory becomes periodic, i.e., traverses its (meanwhile stable) limit cycle. If we start the reversed simulation from somewhere in the vicinity of the unstable limit cycle, the trajectory behavior is extremely sensitive to the precise choice of the initial condition, although, as Fig.8.22 demonstrates, the sensitivity does not have to become evident immediately.

In our example, since both types of simulations tend towards a singular solution, time becomes *irreversible* for all practical purposes if we just wait long enough, i.e., if we perform one type of simulation for sufficiently long and then "forget" the trajectory that we just generated, we cannot hope to retrieve the trajectory by executing the reversed simulation starting from the final value of the original one.

It is true for all (arbitrarily non-linear) systems, that the trajectories are always *repelled* by unstable singularities, and *attracted* by stable singularities. For a long time, it was therefore believed that, if we just wait long enough, all trajectories of autonomous systems do either approach stable singularity points, stable limit cycles, or escape to infinity. This is unfortunately not so. Other types of system behavior exist that are stable, non-stationary, and non-periodic. These are called *chaotic motions*, and we shall analyze examples of such behavior in Chapter 10 of this text.

According to a number of highly reputed physicists, it is this type of time "irreversibility" that is at the origin of the seemingly stochastic microscopic behavior of thermic systems (the Brown movement), and that is ultimately responsible for the irreversibility condition that is expressed in the second law of thermodynamics [8.14]. This rationale was thought to explain the seeming discrepancy between the "time-reversibility" of any state-space model, and the obvious time-irreversibility of thermic systems due to the second law.

However, a much simpler explanation can be found for the time-irreversibility of thermal systems.

Let us look a little more closely at the *physics* of "time-reversal". What does the mathematical operation of inverting the inputs of all integrators mean physically? For this purpose, let us analyze time-reversal in the context of a simple electrical circuit. What does it mean in this context to invert the inputs of all integrators? Let us look at the simple state equation:

$$\frac{du_C}{dt} = \frac{1}{C} \cdot i_C \tag{8.54}$$

Time-reversal transforms this equation into:

$$\frac{du_C}{dt} = -\frac{1}{C} \cdot i_C \tag{8.55}$$

and, since we wish to retain the capacitive current i_C, we need to accept the necessity of a "negative capacitor" which is not exactly a physically sound concept. But let us accept this answer for the time being. "Time-reversal" in a simple passive circuit is accomplished by replacing every capacitor in the circuit by a "negative capacitor", and every inductor by a "negative inductor". If we then let all sources run backward through time, we have achieved the desired time-reversal in terms of the electrical variables, i.e., all voltages and currents in the circuit run "backward" in time.

However, since the currents and voltages over the resistors have not changed after the time-reversal (according to our premises), power is still being dissipated by them, and the resistors continue to heat up rather than cool down (in accordance with the second law). How can we get the thermal variables to reverse as well? Mathematically, the answer is straightforward. We simply must include dissipated energy into our model as an additional state variable, i.e.:

$$\frac{dQ_{irr}}{dt} = P_{elect} = u_R \cdot i_R \tag{8.56}$$

Time-reversal turns this equation into:

$$\frac{dQ_{irr}}{dt} = -P_{elect} = -u_R \cdot i_R \tag{8.57}$$

Unfortunately, this equation is physically simply *wrong*. The dissipated energy is the integral of the electrical power over the resistor, and *not* the integral of the negative electrical power. We could defer

the negative sign to either the resistive voltage or current (by introducing a "negative resistance"), but this would not be in accordance with the time–reversal of the electrical variables.

What we learned is the fact that the operation of "simply placing an inverter in front of every integrator in the system" is not a physically meaningful proposition. This is exactly what I meant when I wrote in Chapter 1 of this book about the danger of "falling in love with our model". Many mathematically correct manipulations can be applied to a model, which could never be applied to the real system because they violate its physicality conditions. Therefore, the mathematically feasible time–reversal of state–space models is not in contradiction with the second law of thermodynamics. The facts are much simpler than that. The mathematical operation of "time–reversal" simply violates the physicality of the model.

8.7 Summary

In this chapter, we have discussed thermodynamics from a systemic rather than from a phenomenological view point. We have seen that bond graphs present us with a tool to ensure adherence to physicality in modeling thermodynamic systems, and we have seen by means of an extended (drastic) example what can happen if physicality is being ignored in the process of model manipulations. Bond graphs are *not* just another tool for mathematical modeling. In fact, bond graphs are quite meaningless when applied to the description of mathematical equations bare of their physical interpretation. It is therefore not currently feasible to apply bond graphs to the description of a macro–economic model, for example, since we don't know what "energy conservation" means in such a model. What means "economic power" in a system theoretical rather than in a political sense? We don't know. Consequently, we cannot define a set of adjugate variables that describe the behavior of a macro–economy.

However, I would like to go one step further. While I cannot prove this to be correct, I am personally convinced that any real system, that can meaningfully be described by a differential equation model (and macro–economic systems are among those without any question), possesses some sort of "energy" which obeys the law of energy conservation. It is just that, to my knowledge, nobody ever has looked into systems, such as macro–economies, from quite that perspective, and has tried to come up with a meaningful and consistent

definition of the terms "energy" and "power", and from there has derived a set of adjugate variables, the product of which is "power". This would be a very worthwhile topic for a Ph.D. dissertation.

Bond graphs have been successfully applied to most areas of physical systems which result in ordinary differential equation models. In this chapter, we have seen a meaningful application of bond graphs to one case of a partial differential equation as well, namely the diffusion equation eq(8.2). However, bond graphs have not yet been successfully applied to most other types of PDE models such as those occurring in fluid dynamics [8.3,8.4]. The reason is again a simple one. Most systems that are governed by PDE's require more than just energy conservation. Liquids can change their shape while they still preserve their volume. Gases don't even preserve their volume. Yet, all these systems conserve *mass*. Consequently, we must ensure that our models not only conserve energy, but also that they conserve mass. In a bond graph, mass appears as a parameter. Distributed pneumatic systems would therefore have to be described through modulated parameters, a technique which does not guarantee that the mass is properly conserved. It is currently unclear how we can come up with a systematic methodology, a *generalized bond graph* maybe, that ensures conservation of both energy and mass simultaneously. Such an investigation might therefore be a fruitful topic for yet another Ph.D. dissertation — not exactly an easy task either. I shall pursue this avenue quite a bit further in Chapter 9, but the final answer to this question has certainly not yet been given.

Please, notice that the theoretical foundations from which the bond graph methodology was derived are much deeper than I was willing to reveal in this book. In particular, notice the similarity between the concept of "adjugate variables" as used in the bond graph approach to the modeling of physical systems, and the "adjugate variables" that were briefly introduced in Chapter 4 relating to the Hamiltonian of a system, and yet, the Hamiltonian was only defined for conservative (i.e., non–dissipative) systems, while bond graphs extend naturally to cover dissipative processes as well. This similarity is not accidental and needs to be explored further. The question of finding a "generalized bond graph" may be just another formulation of the desire to find a "generalized Hamiltonian", a hot topic among applied mathematicians who are interested in the study of dynamical systems.

Finally, I would like to acknowledge the contributions of Peter Breedveld of the Technical University Twente (Enschede, The Netherlands). His insight into the principles of thermodynamics and

into the bond graph methodology, as expressed in his Ph.D. dissertation [8.1], were essential to my understanding of the material presented in this chapter.

References

[8.1] Peter C. Breedveld (1984), *Physical Systems Theory in Terms of Bond Graphs*, Ph.D. Dissertation, Technical University Twente, Enschede, The Netherlands.

[8.2] François E. Cellier (1990), "Hierarchical Non-linear Bond Graphs — A Unified Methodology for Modeling Complex Physical Systems", Keynote Address, *Proceedings European Simulation MultiConference*, Nürnberg, FRG, pp. 1–13.

[8.3] N. Curle, and Hubert J. Davies (1968,1971), *Modern Fluid Dynamics*, two volumes, Van Nostrand Reinhold, London, U.K.

[8.4] Iain G. Currie (1974), *Fundamental Mechanics of Fluids*, Mc Graw Hill, New York.

[8.5] John A. Duffie, and William A. Beckman (1980), *Solar Engineering of Thermal Processes*, John Wiley, New York.

[8.6] International Colloquium on Field Simulation (1976), Proceedings of the Fourth International Colloquium on the Beuken Model, September 1974, Polytechnic of Central London, London, U.K.

[8.7] Aharon Katzir-Katchalsky, and Peter F. Curran (1965), *Nonequilibrium Thermodynamics in Biophysics*, Harward University Press, Cambridge, MA.

[8.8] Bernard H. Lavenda (1985), *Nonequilibrium Statistical Thermodynamics*, John Wiley, New York.

[8.9] Derek F. Lawden (1987), *Principles of Thermodynamics and Statistical Mechanics*, John Wiley, New York.

[8.10] Fritz London (1954), *Superfluids – Volume II: Macroscopic Theory of Superfluid Helium*, John Wiley, New York.

[8.11] V. Peshkov (1944), " 'Second Sound' in Helium II", *J. Phys. USSR*, **8**, p.381.

[8.12] V. Peshkov (1946), "Determination of the Velocity of Propagation of the Second Sound in Helium II", *J. Phys. USSR*, **10**, pp. 389–398.

[8.13] Ilya Prigogine (1967), *Thermodynamics of Irreversible Processes*, Third Edition, John Wiley Interscience, New York.

[8.14] Ilya Prigogine (1980), *From Being to Becoming: Time and Complexity in the Physical Sciences*, Freeman, San Francisco, CA.

[8.15] Keith S. Stowe (1984), *Introduction to Statistical Mechanics and Thermodynamics*, John Wiley, New York.

[8.16] Jean U. Thoma (1975), "Entropy and Mass Flow for Energy Conversion", *J. Franklin Institute*, **299**(2), pp. 89–96.

[8.17] Clifford Truesdell (1984), *Rational Thermodynamics*, Second Edition, Springer, New York.

[8.18] Y. L. Yao (1981), *Irreversible Thermodynamics*, Science Press, Beijing, distributed by: Van Nostrand Reinhold, New York.

Bibliography

[B8.1] A. M. Bos, and Peter C. Breedveld (1985), "Update of the Bond Graph Bibliography", *J. Franklin Institute*, **319**(1/2), pp. 269–286.

[B8.2] Vernon D. Gebben (1979), "Bond Graph Bibliography", *J. Franklin Institute*, **308**(3), pp. 361–369.

Homework Problems

[H8.1] Heat Flow Along a Copper Rod

A copper rod of length $\ell = 1\ m$ and radius $r = 0.01\ m$ is originally in an equilibrium state at room temperature $T = 298.0°K$. At time $t = 0.0\ sec$, the left end of the rod is brought in contact with a body which is kept at a temperature of $T_L = 390.0°K$.

Model the rod through a set of 10 one–dimensional cells. Model the boundary conditions through an effort source attached to the input port of the first segment, and specify that the heat flow out of the output port of the last segment is zero. We want to assume that the heat transport in the rod occurs purely by means of diffusion, and that the rod is so well insulated that no heat escapes through its surface.

The density of copper is $\rho = 8960.0\ kg\ m^{-3}$, the specific thermal conductance is $\lambda = 401.0\ J\ m^{-1}\ sec^{-1}\ °K^{-1}$, and the specific thermal capacitance is $c = 386.0\ J\ kg^{-1}\ °K^{-1}$.

Simulate the system during 20000.0 *sec*, and display the temperature in the middle of the rod and at the end of the rod.

[H8.2] Lightning Rod

A copper lightning rod of length $\ell = 5\ m$ and radius $r = 0.01\ m$ is originally in an equilibrium state at room temperature $T = 298.0°K$. At time $t = 0.0\ sec$, the left end of the rod is hit by lightning which results in a current flow of $I_0 = 200\ kA$ which lasts for a duration of $t_{pulse} = 75\ \mu sec$.

Model the rod through a set of 10 one–dimensional cells with *RS* elements attached to each cell which represent the heat input through electrical dissipation. Model the boundary conditions through a flow source attached to the single electrical port, and specify that the heat flow out of the output port of the last cell is zero. We want to assume that the heat transport in the rod occurs purely by means of diffusion, and that the rod is so well insulated that no heat escapes through its surface.

The density of copper is $\rho = 8960.0\ kg\ m^{-3}$, the specific thermal conductance is $\lambda = 401.0\ J\ m^{-1}\ sec^{-1}\ {}^{\circ}K^{-1}$, the specific thermal capacitance is $c = 386.0\ J\ kg^{-1}\ {}^{\circ}K^{-1}$, and the specific electrical resistance is $\rho_{el} = 1.7 \cdot 10^{-8}\ \Omega\ m$.

Simulate the system during $5 \cdot 10^{-4}\ sec$, and display the temperature in the middle of the rod and at the end of the rod. Which is the maximum temperature increase that the lightning rod experiences?

Projects

[P8.1] Solar Heated House

Fig.P8.1a depicts a solar heated house. One or several collectors act as black bodies which absorb incoming solar radiation. Consequently, the temperature inside the collectors raises. The collectors can be filled with any material with a large heat capacity. Usually, it is simply air. Inside the collectors, a water pipe meanders back and forth between the two ends of the collector thereby maximizing the exposed pipe surface. We shall call this a "water spiral" [8.2]. A (mostly conductive) heat exchange takes place between the collector chamber and the water pipe, thereby heating the water in the pipe. A pump circulates the water from the collectors to the storage tank, thereby transporting the heat convectively from the collectors to the tank. We call this the "collector water loop" [8.2]. The water spirals in the various collectors can be either series connected, or they can be connected in parallel. The pump is usually driven by a solar panel. In the panel, the solar light is converted to electricity which drives the pump. Thereby, the pump circulates the water only while the sun is shining which is exactly what we want. In addition, a freeze protection device is often installed which also switches the pump on whenever the outside temperature falls below $5°C$.

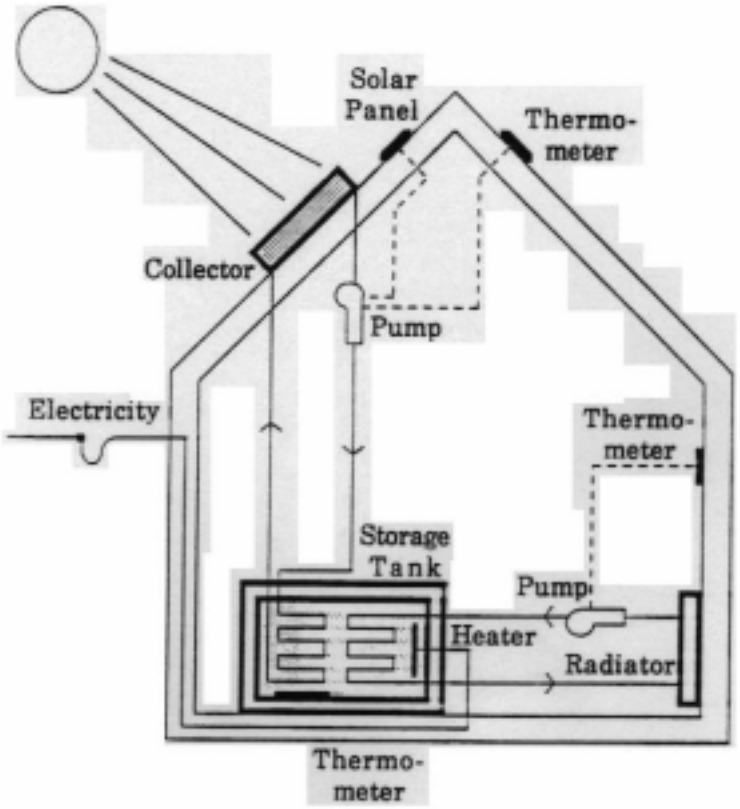

Figure P8.1a. A solar heated house

The storage tank is often realized simply as a large and well insulated water container (a water heater). However, such a solution would get us into mixing thermodynamics, and may be a little difficult to model at this point. Therefore, we shall assume that a solid body storage tank is used together with another water spiral which deposits the heat in the storage tank just the same way as it was picked up in the collectors. Consequently, the water from the collector loop and from the heater loop never mix.

A second water spiral inside the storage tank belongs to the "heater water loop". It picks up the heat from the storage tank. An additional electrical heater is also installed which heats the storage tank electrically whenever the storage tank temperature falls below a critical value, but does so only during night hours when electricity is cheap.

The heater water loop is driven by another pump which is switched on whenever the room temperature falls below $20°C$ during the day or $18°C$

during the night, and which is switched off whenever the room temperature raises beyond $22°C$ during the day or $20°C$ during the night.

In the house, we use one or several "radiators" (more water spirals) which, contrary to what their name suggests, exchange heat with the room in a partly conductive and partly convective manner.

Fig.P8.1b depicts the collector in more detail.

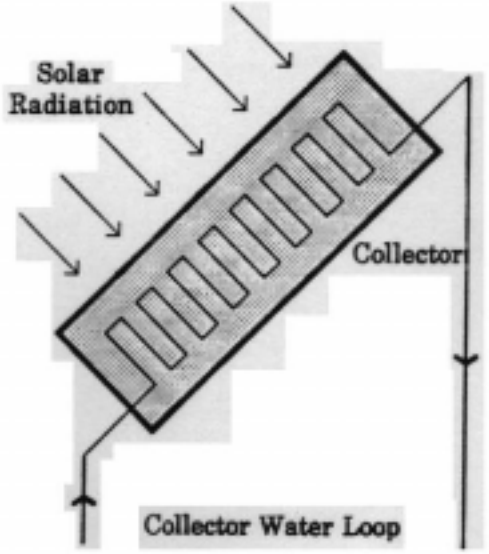

Figure P8.1b. The solar collector

The water spiral is modeled through a series of one–dimensional cells as introduced in this chapter. We want to model each such cell as shown in Fig.P8.1c.

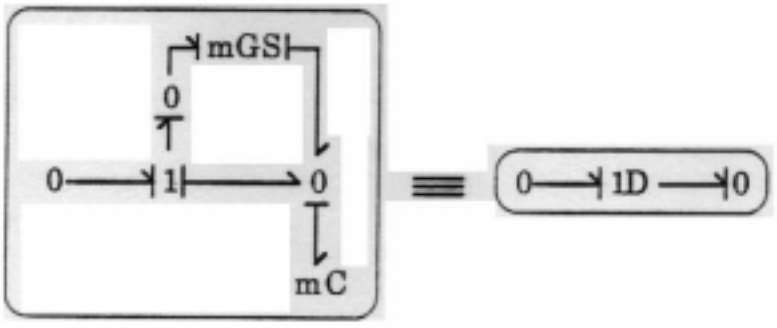

Figure P8.1c. Bond graph of a one–dimensional cell

Each cell is described by a DYMOLA model type called *c1d.dym* which, from now on, can be used as an additional bond graph element. The correct causalities have been marked on the graph. The *mGS* element is a "modulated conductive source". It is modulated with temperature (as always in thermal systems), but, in addition, it is also modulated with the water velocity in the pipe as shown in Fig.P8.1d. Since the conductance changes linearly with the water velocity v_w, it was preferred to model this element through its conductance rather than through its resistance.

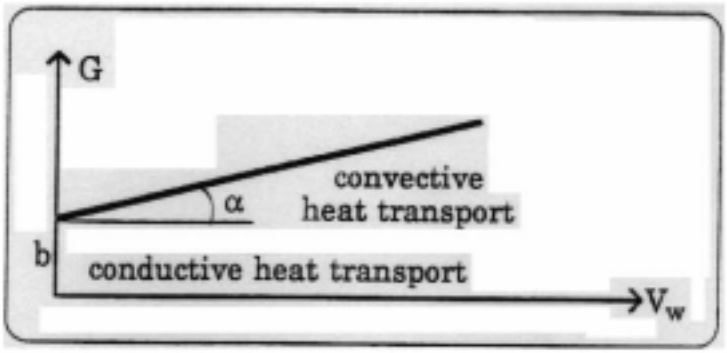

Figure P8.1d. Modulated conductive source

The *c1d* model references three submodels, a temperature modulated capacitance *mC*, a temperature and water velocity modulated conductive source *mGS*, and finally the regular *bond* submodel. Remember to augment the bond graph by additional 0–junctions to ensure that all elements are attached to 0–junctions only.

Fig.P8.1e shows the heat exchanger model which is used to describe the exchange of heat across the border of two media.

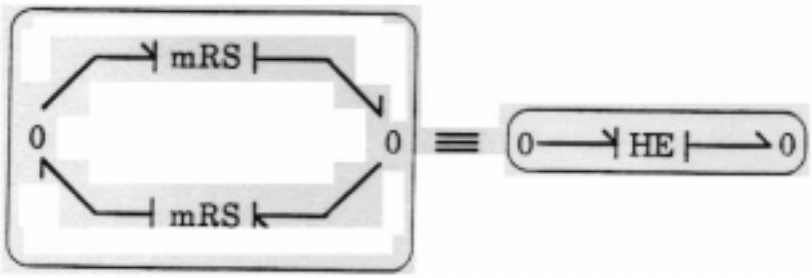

Figure P8.1e. Bond graph of a heat exchanger

The heat exchanger is used here to model the transfer of heat from the collector chamber to the water spiral.

The water spiral is modeled through a series connection of several *c1d* elements with heat exchangers attached in between. Fig.P8.1f shows the water spiral. We decided to cut the spiral into three discrete links. Obviously, this is an approximation of a process with distributed parameters.

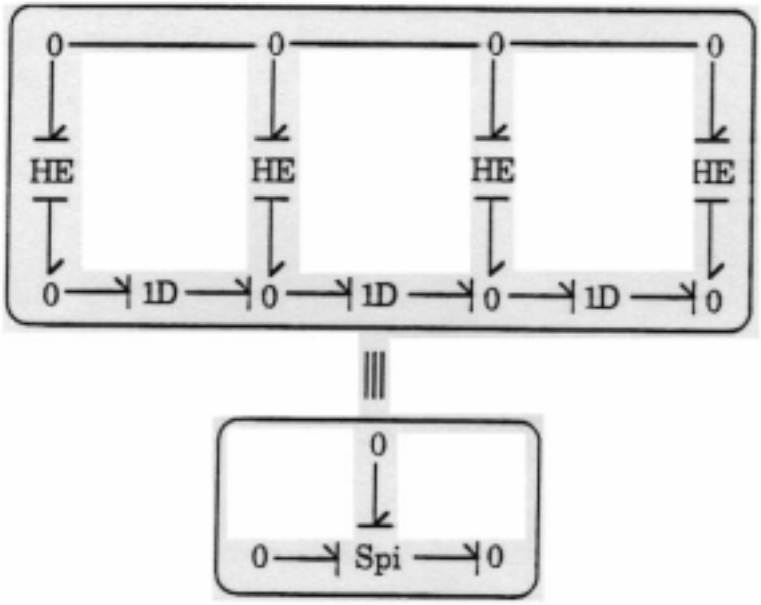

Figure P8.1f. Bond graph of a water spiral

Notice that the newly introduced bond graph symbol representing the water spiral is a *3-port element.*

We need to model also the loss from the collector chamber to the environment. This loss is partly conductive and partly convective. Fig. P8.1g depicts the loss element (a 1-port element).

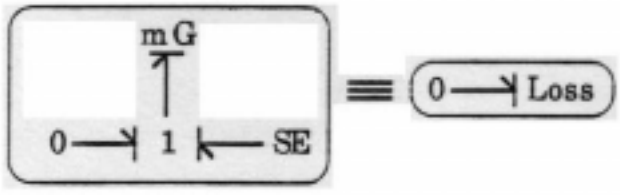

Figure P8.1g. Bond graph of thermic loss

The effort source denotes the outside temperature. The *mG* element denotes the heat dissipation to the environment. The dissipated heat is proportional to the difference in temperatures between the inside and the outside. *mG* is a modulated conductance similar to the *mGS* element found earlier, but this time, the secondary port (the environment) is not modeled, and the modulation is now with respect to the wind velocity v_{wind} rather than with respect to the water velocity v_w.

We are now ready to model the overall collector. Fig.P8.1h shows the overall collector.

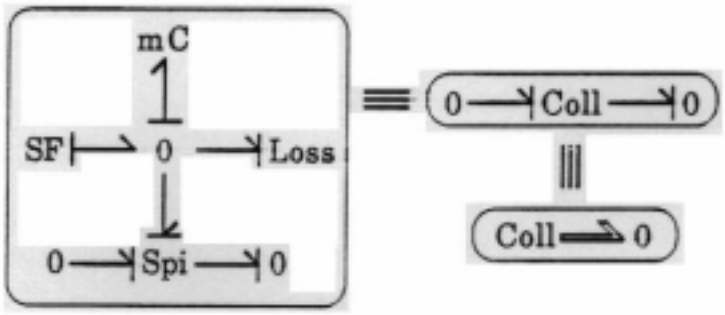

Figure P8.1h. Bond graph of the collector

The *mC* element is the (temperature modulated) heat capacitance of the collector chamber. The *SF* element denotes the heat input from solar radiation.

We use the hierarchical cut concept of DYMOLA to combine the two cuts (i.e., bonds), *inwater* and *outwater*, into one hierarchical cut, *water*. This can be pictorially represented by a double bond. This *aggregated bond graph representation* has, of course, the disadvantage that causalities can no longer be depicted.

Let us now model the heat input from the solar radiation. Fig.P8.1i shows a typical heat flow curve over a period of three days.

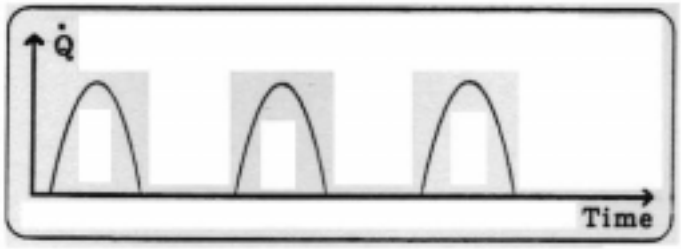

Figure P8.1i. Heat flow from solar radiation

Of course, the curve changes somewhat with the time of the year and with the location on the globe (the latitude). We wish to model the heat flow correctly for an arbitrary time of the year, and for an arbitrary latitude. For this purpose, create a model that describes the motion of planet Earth around the sun. Neglect the influence of the moon and of the other planets. The output of that model will be the celestial coordinates (declination and right ascension) of planet Earth as a function of the time of the year expressed in sun–centered coordinates. Create a second model that converts these coordinates to the celestial position of the sun expressed in Earth–centered coordinates. Create a third model that, for any position on our globe, converts the celestial coordinates into surface–bound coordinates, i.e., use the sidereal time to convert the right ascension of the sun to its hour angle equivalent.

By now, we know the apparent position of the sun for any latitude, for any day of the year, and for any time of the day. We need to convert this to the available solar heat flow. This depends on the angle of the sun above the horizon, or more precisely, it depends on the thickness of the atmospheric layer that the solar rays must travel through before reaching the surface. This function has been tabulated and can be found in the literature. Create a model that converts the solar position to the available heat flow (assuming optimal visibility and a spotless blue sky).

At this point, we know how much solar heat is available per time unit and per visible unit surface. The visible surface of the collector depends on its physical surface and on its position. Let us assume that we operate with one flat collector. We shall certainly position the collector exactly towards the south when located anywhere on the northern hemisphere, and exactly towards the north when located on the southern hemisphere. The optimal slanting angle with the horizontal depends on the latitude. At the equator, the optimal angle is 0°, at the pole it is 90°. It turns out that a good choice for the slanting angle is the latitude itself. Standard collectors come in sizes of 1 $m \times 2$ m. Create a model that converts the available solar heat to effectively used solar heat per optimally positioned but fixed flat collector at any given latitude, at any given day of the year, and at any given time of the day.

Since heat flow is the product of entropy flow and temperature, we can divide the effectively used heat by the collector temperature, and model the resulting entropy flow into the collector as a (time and temperature modulated) heat source.

We are now ready to model the transport of heat from the collector to the storage tank, i.e., the collector water loop. We model each of the pipes through a series of one–dimensional cells, and we shall assume that the pipes are thermically well insulated, i.e., that no heat is lost to the environment on the way. Fig.P8.1j depicts the water loop.

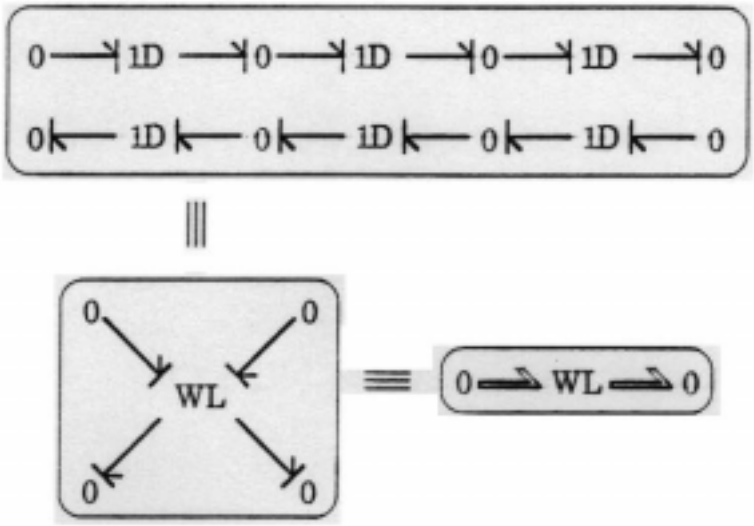

Figure P8.1j. Bond graph of the water loop

This bond graph element is a 4–port. We shall combine the cut *inwater1* with the cut *outwater2* to the hierarchical cut *inwater*, and the cut *outwater1* with the cut *inwater2* to the hierarchical cut *outwater*. We shall furthermore declare a main path *water* which creates a logical bridge from the hierarchical cut *inwater* to the hierarchical cut *outwater*.

The storage tank contains two water spirals, one which belongs to the collector water loop, and one which belongs to the heater water loop. In addition, an electrical resistance heater has been installed as a backup device. The electrical heater is turned on only if the temperature in the storage tank falls below a critical value. Furthermore, the backup device is never used during day–time hours when the electricity is expensive, instead, we shall wait with electrically heating the storage tank until the evening hours when the price for electricity is lower. Fig.P8.1k shows the storage tank.

The mC element denotes the heat capacity of the storage tank. The flow source together with the mRS element denote the electrical backup heater. The primary side of the resistive source is electrical while the secondary side is thermic.

This is another 4–port. This time, we shall combine the cut *inwater1* with the cut *outwater1* to the hierarchical cut *inwater*, and the cut *outwater2* with the cut *inwater2* to the hierarchical cut *outwater*. We shall again declare a main path *water* which creates a logical bridge from the hierarchical cut *inwater* to the hierarchical cut *outwater*.

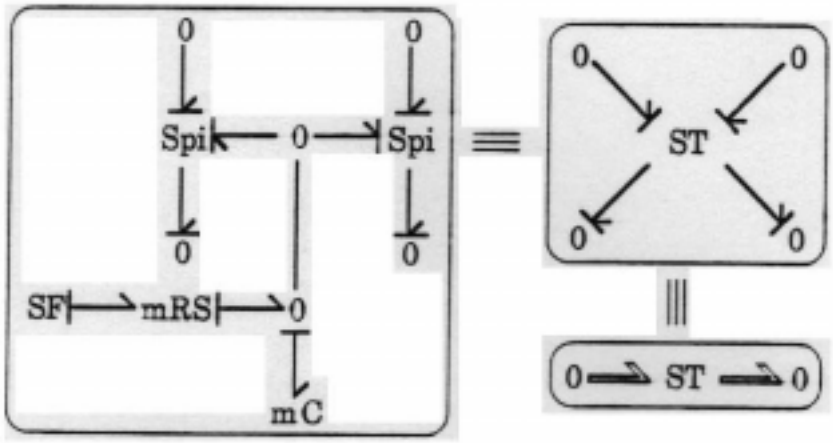

Figure P8.1k. Bond graph of the storage tank

The heater water loop is modeled in exactly the same manner as the collector water loop.

Finally, let us discuss the house itself. For simplicity, we shall assume that the house is a cube of 10 m x 10 m x 10 m. We shall model the house with 27 three-dimensional cells, three in each direction. Let us assume that the entire house consists of one room only, and that a single (large) radiator is used to heat the house. The radiator is attached to the left wall of the house somewhere close to the floor, i.e., heat input occurs at the left low outside center 3d–cell. We shall not model the radiator explicitly since it is much smaller in dimensions than the house itself. Therefore, we shall simply connect the *outwater1* of the heater water loop with the *inwater2* of the heater water loop. At this node, we attach another heat exchanger which is responsible for the exchange of heat between the heater water loop and the house.

We shall also assume that the house loses some heat through the four walls and through the roof, but not through the floor. Attach *Loss* elements to each of the 0–junctions as appropriate. If a cell is adjacent to two or three outside walls, attach one combined loss element to the corresponding node only since otherwise an algebraic loop will occur.

This concludes the description of the system. Fig.P8.1l depicts the overall system as a series connection of the previously presented aggregated bond graph elements.

Figure P8.11. Aggregated bond graph of the overall system

Since, in a solar heating system, we pay for the installed energy rather than for the utilized energy, such a heating system is only economical in a climate with extended heating periods combined with lots of sunshine. Let us assume that our solar house is situated in Denver, Colorado. We wish to analyze the effectiveness of our heating system. For this purpose, we study the behavior of our heating system for December 21, the beginning of winter. The sun shines from a spotless blue sky. The outside temperature is time dependent. The time dependence can be modeled with a sine function. The low temperature is $-10°C$. It is reached at 3 *a.m.* The high temperature is $+5°C$. It is reached at 3 *p.m.*

We first want to determine the critical temperature of the storage tank. For ths purpose, we simulate the heating of the house with a constant storage tank temperature. Let us assume that our initial temperature in the house is $15°C$. We should be able to heat the house to $20°C$ within four hours. Determine the size of the radiator (i.e., the conductance of the heat exchanger between the heater water loop and the house), and an appropriate storage tank temperature which will allow you to attain this goal. Of course, the smaller you choose the radiator, the higher must be the storage tank temperature. You can find decent values in Duffie and Beckman [8.5]. This will thus determine our critical temperature.

Next, we want to dimension the electrical backup system. The electrical heater should be able to raise the storage tank temperature from room temperature, i.e. $20°C$, to the critical temperature within one hour.

Next, we want to dimension the collector system. Determine how many of the (series connected) standard collectors are required to keep the storage tank temperature at a periodic steady state for the December 21 situation without activating the backup heating device.

Many parameter values must be selected. Use recommended values from the literature [8.5] where available, otherwise use physical intuition and common sense to determine appropriate values for these parameters. Simulate the overall system for various climatic conditions. Use published weather data to determine the frequency of utilization of the electric backup system. What is the reduction in the utility bill achievable with this system in comparison with an electric only solution? Simulate the electric only solution by permanently disabling the collector water loop pump.

Research

[R8.1] Second Sound Wave in Superfluid Helium–II

Formulate the two–fluid theory, which explains the behavior of liquid Helium in the vicinity of the so–called λ–point, in terms of a bond graph. Come up with a simulation model that reproduces the observed second sound wave while conserving both energy and mass in the system.

[R8.2] Bond Graphs for Maxwell's Equations, Non–linear Optics, and Fluid Dynamics

In this chapter, we have shown one successful application of bond graphs for modeling distributed parameter systems. For the reasons explained in the summary section, other types of PDE problems don't lend themselves as easily to a bond graph formulation. The simplest other type of practical PDE problem is the wave equation:

$$\frac{\partial^2 u}{\partial t^2} = c^2 \cdot \frac{\partial^2 u}{\partial x^2} \qquad (R8.2a)$$

$$\frac{\partial^2 i}{\partial t^2} = c^2 \cdot \frac{\partial^2 i}{\partial x^2} \qquad (R8.2b)$$

which can describe the transport of voltage and current along a lossless transmission line, the pressure and flow rate of a compressible liquid or gas in a pipe, the longitudinal oscillation of an elastic rod, sound waves in gases or liquids, and optical waves.

Also the wave equation can be modeled easily in terms of an equivalent electrical circuit, and therefore, in terms of a bond graph. Fig.R8.2a shows the equivalent electrical circuit:

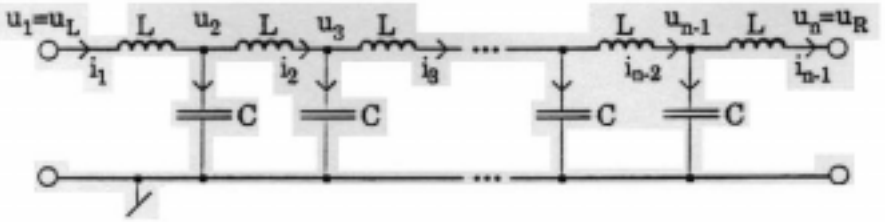

Figure R8.2a. Equivalent electrical circuit modeling the wave equation

and Fig.R8.2b shows a corresponding bond graph:

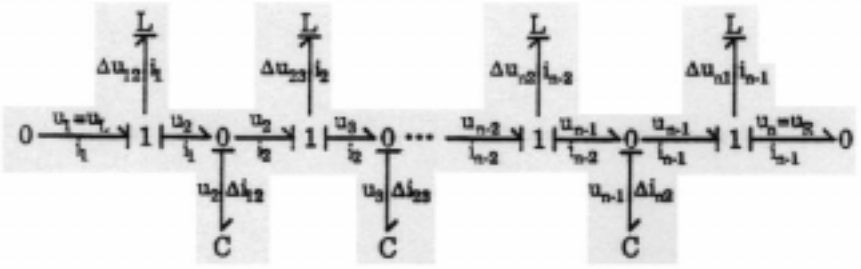

Figure R8.2b. Bond graph for the wave equation

The variables are specified for an electromagnetic wave.

Unfortunately, this brings us to the end of the simple analogies. Problems in electromagnetics and non–linear optics are probably a little easier to tackle than those in fluid dynamics since we don't need to concern ourselves with an additional equation (the mass conservation equation), and yet, already these problems are quite tough.

Let us look at a fairly simple problem, the electrical transmission line with dissipative losses. This system can be modeled by the telegraph equation:

$$\frac{\partial^2 u}{\partial x^2} = RGu + (RC + LG)\frac{\partial u}{\partial t} + LC\frac{\partial^2 u}{\partial t^2} \qquad (R8.2c)$$

$$\frac{\partial^2 i}{\partial x^2} = RGi + (RC + LG)\frac{\partial i}{\partial t} + LC\frac{\partial^2 i}{\partial t^2} \qquad (R8.2d)$$

where:

$$Z_{sh} = R + sL \qquad (R8.2e)$$

is the impedance of a unit length segment of the short–circuited transmission line, and:

$$Y_{op} = G + sC \qquad (R8.2f)$$

is the admittance of a unit length segment of the open transmission line. An approximate solution can be found by combining the bond graph of Fig.R8.2b with that of Fig.8.10, i.e. by adding *RS*–elements to the bond graph of Fig.R8.2b. However, this bond graph does not model the telegraph equation exactly. It is possible to add *RS*–elements emanating from the 1–junctions and *GS*–elements emanating from the 0–junctions without introducing algebraic loops, but it is not clear that this will bring much of

an improvement. On the other hand, if we solve a PDE problem numerically, we discretize anyway, and therefore approximate the true distributed parameter system by a lumped parameter system. It is not clear that the above proposed circuit analogy is worse than any other approximation that we may choose.

Fluid dynamics problems are governed by the Navier–Stokes equation (for the energy balance) combined with an additional equation (for the mass balance). These are tough problems to solve. A bond graph model that shows how the energies and masses flow through the system would indeed be very useful. I am convinced that any good numerical algorithm ought to take energy and mass flows into consideration, and should try to map into a numerical scheme what the physics dictate in the real system, not only in the overall solution, but also in the implementation of individual steps.

[R8.3] Bond Graphs for Macro–Economies

Define a set of adjugate variables for models of macro–economic systems together with a formulation of the energy conservation law as applied to these adjugate variables. Show, by means of examples, how this concept can be used to model macro–economic systems.